Thermodynamic Stability of the P4−P6 Domain RNA Tertiary Structure Measured by Temperature Gradient Gel Electrophoresis†

Alexander A. Szewczak,‡ Elaine R. Podell, Philip C. Bevilacqua,§ and Thomas R. Cech*

Howard Hughes Medical Institute, Department of Chemistry and Biochemistry, University of Colorado, Boulder, Colorado 80309-0215

Received March 19, 1998; Revised Manuscript Received May 27, 1998

ABSTRACT: The P4−P6 domain RNA from the *Tetrahymena* self-splicing group I intron is an independent unit of tertiary structure that, in the kinetic folding pathway, folds before the rest of the intron and then stabilizes the remainder of the intron's tertiary structure. We have employed temperature gradient gel electrophoresis (TGGE) to examine the unfolding of the tertiary structure of P4−P6. In 0.9 mM Mg^{2+}, the global tertiary fold of the molecule has a melting temperature of approximately 40 °C and is completely unfolded by 60 °C. Calculated thermodynamic parameters for folding of P4−P6 are $\Delta H^{\circ\prime} = -28 \pm 3$ kcal/mol and $\Delta S^{\circ\prime} = -91 \pm 8$ eu under these conditions. Chemical probing of the P4−P6 tertiary structure using dimethyl sulfate and CMCT confirms that these TGGE experiments monitor the unfolding of the global tertiary fold of the domain and that the secondary structure is largely unaffected over this temperature range. Thus, unlike the entropically driven P1 docking and guanosine binding steps of *Tetrahymena* group I intron self-splicing, which have positive or zero ΔH terms, P4−P6 tertiary structure formation is stabilized by a negative ΔH term. This implies that enthalpically favorable hydrogen bond formation, nucleotide base stacking, and/or binding of Mg^{2+} within the folded structure are responsible for stabilizing the P4−P6 domain.

In addition to acting as a medium for transmission of genetic information, ribonucleic acids often perform or contribute to biological catalysis, for example in splicing and translation (*1*). Of primary importance to the function of each RNA is the specific three-dimensional shape of the molecule that properly configures functional groups for binding or catalysis. Understanding how RNA achieves its shape is roughly analogous to the protein folding problem (*2*−*5*). Recently, the determination by X-ray crystallography of the structure of a large ribonucleic acid, the P4−P6[1] domain from the *Tetrahymena* self-splicing group I intron, revealed a wealth of detailed information about interactions that stabilize higher order RNA structure (*6*−*8*).

The P4−P6 RNA component of the *Tetrahymena* group I intron is an independently folding domain of tertiary structure stabilized by Mg^{2+} (*9, 10*). In addition to forming part of the catalytic core of the molecule (*11*), it has been shown to stabilize the intron (*12*−*14*) and to nucleate the folding pathway of the intron's tertiary structure (*3, 15*−*18*). In fact, without the P4−P6 domain, the intron is inactive. However, when the isolated P4−P6 domain is added *in trans*, it stably associates with the rest of intron and rescues activity (*19*). We have been using the P4−P6 domain as a model system to study RNA folding by examining the interactions that stabilize its three-dimensional structure and determining their energetic contributions. Formation of the independent P4−P6 tertiary structure has been extensively studied using a wide variety of techniques, including chemical modification and Fe(II)−EDTA-based hydroxyl radical cleavage (*9, 10, 20, 21*), oligonucleotide-directed RNase H cleavage (*3, 15*), and electron microscopy (*20*). In addition, P4−P6 folding can be observed using native gel electrophoresis (*20, 22*).

The isolated P4−P6 domain tertiary structure is made up of two components, both of which require Mg^{2+} ions to form. The P5abc extension forms a stable subdomain structure with a $[Mg^{2+}]_{1/2}$ of about 0.5 mM. The larger, more global, three-dimensional fold of the molecule forms in 1 mM Mg^{2+} (*10, 21*). On native polyacrylamide gels this fully folded form of the molecule migrates substantially faster than the unfolded form consisting of only the subdomain tertiary structure (*20*). Previous experiments have suggested that under certain conditions the P4−P6 domain is in equilibrium between folded and unfolded states and that its gel mobility measured relative to an control molecule which cannot fold, BP 5/5a, is a measure of the fraction of molecules folded (*22*). In light of this, we reasoned that we might use

† Supported by the Howard Hughes Medical Institute. T.R.C. is an Investigator of the Howard Hughes Medical Institute and an American Cancer Society Professor. A.A.S. was the recipient of a fellowship from the Jane Coffin Childs Memorial Fund for Medical Research. P.C.B. was an Associate of the Howard Hughes Medical Institute.

* To whom correspondence should be addressed. Phone: (303) 492-8606. Fax: (303) 492-6194. E-mail: Thomas.Cech@Colorado.EDU.

‡ Current address: Department of Molecular Biophysics and Biochemistry, Yale University, New Haven, CT 06520.

§ Current address: Department of Chemistry, The Pennsylvania State University, University Park, PA 16802.

[1] Abbreviations: BP 5/5a, mutated version of the P4−P6 domain RNA that is base paired in the region between P5 and P5a; CMCT, *N*-cyclohexyl-*N*′-[2-(*N*-methyl-4-morpholino)ethyl]carbodiimide-4-toluenesulfonate; DMS, dimethyl sulfate; DTT, dithiothreitol; EDTA, ethylenediaminetetraacetic acid; HEPES, 4-(2-hydroxyethyl)-1-piperazineethanesulfonic acid; P4−P6, the *Tetrahymena* group I intron domain which contains helices P4, P5, P5a, P5b, P5c, P6, P6a, and P6b; TGGE, temperature gradient gel electrophoresis; THE, Tris−HEPES−EDTA buffer; Tris, tris(hydroxymethyl)aminomethane.

S0006-2960(98)00633-3 CCC: $15.00
Published on Web 07/21/1998

temperature gradient electrophoresis to analyze the melting behavior of the P4−P6 domain structure.

In temperature gradient gel electrophoresis (TGGE) molecules travel across a linear temperature gradient applied either in parallel with, or perpendicular to, the electric field. In a predecessor to this method, a gradient of urea in a gel was used to provide a progressively destabilizing environment (*23*−*25*). In contrast, TGGE allows observation of gel mobility as a direct function of increasing temperature and was originally used to study protein denaturation (*26*, *27*). Subsequently, TGGE has been applied to a variety of problems, including the analysis of sequence variation in large nucleic acids, conformational transitions in viroid RNAs, and protein−nucleic acid interactions (*28*−*30*). In this work we extend the use of temperature gradient gel electrophoresis to the analysis of the thermodynamics of tertiary structure formation in RNA. Using the P4−P6 system, we are able to observe tertiary structure melting transitions relative to an unfolded control and from them extract thermodynamic parameters for the formation of the P4−P6 domain structure.

EXPERIMENTAL PROCEDURES

RNA Preparation. Plasmids encoding the sequence for the mutant BP 5/5a (*21*) or wild-type P4−P6 (*10*) were digested with *Ear*I restriction endonuclease and transcribed using T7 RNA polymerase. The runoff transcripts (160 nt) begin with two Gs 5′ of the naturally occurring nucleotide A104 and end at A261 of the *Tetrahymena* group I sequence. T7 RNA polymerase transcription, gel purification, dephosphorylation, and subsequent 5′ ^{32}P-end labeling of these RNAs were performed as described (*22*, *31*). Following the labeling reactions, RNAs were again gel purified on 8% polyacrylamide−7 M urea gels. RNA concentrations were measured by UV absorbance, assuming 1 A_{260} = 40 μg/mL RNA.

Temperature Gradient Gel Electrophoresis. Experiments were carried out on a custom-built apparatus similar to one previously described (*28*). The nondenaturing 8% polyacrylamide gels (19:1 acrylamide:bisacrylamide) and running buffer used for temperature gradient gel electrophoresis contained 34 mM Tris, 66 mM HEPES (pH 7.4), 0.1 mM EDTA (1× THE), and 10 mM NaCl ("TGGE buffer") plus varying concentrations of $MgCl_2$, depending on the experiment. To ensure that BP 5/5a and wild-type P4−P6 were in their proper native conformations at the start of each experiment, the RNAs were renatured in the same tube by heating for 10 min at 55 °C in a 185 μL volume of TGGE buffer, $MgCl_2$, and 5% glycerol, followed by cooling on the bench for at least 10 min. Immediately before loading, 5 μL of a 1% solution of xylene cyanol and bromophenol blue marker dyes was added to the samples. In addition, because of convection currents in the well, another 10 μL of 50% glycerol was added to the samples to facilitate loading.

A typical TGGE experiment was conducted as follows: The temperature gradient gel apparatus was connected to two externally circulating temperature baths, one equilibrated at 0 °C and the other at 65 °C, configured to create a horizontal temperature gradient perpendicular to the applied field. Each gel was prerun with the desired temperature gradient for 45 min before the RNA samples were loaded. The gradient ranged from about 14 to about 60 °C in the gel itself, and at the completion of each TGGE experiment actual temperatures within the gel matrix were measured using a Fluka multimeter connected to a thermocouple module with a long probe that fit within the 1.5 mm gel spacers. Each gel was run at constant voltage (260 V) for about 2.5 h, then dried on Whatman 3M paper, and analyzed using a PhosphorImager (Molecular Dynamics).

Thermodynamic Calculations. Assuming a two-state model for the rapid interconversion of folded and unfolded forms of P4−P6 RNA (*18*, *22*), intermediate gel mobilities can be interpreted as the linear combination of the intrinsic mobilities of the folded and unfolded forms of the molecule, scaled by the fraction of the population of RNA in each state. This is analogous to the technique used to analyze nucleic acid UV melting curves (*32*, *33*). Hence, the fraction folded as a function of temperature, $\alpha(T)$, can be calculated as $[D_X(T) - D_U(T)]/[D_F(T) - D_U(T)]$, where $D_X(T)$ = the distance migrated for a band "x" of intermediate mobility, and $D_U(T)$ and $D_F(T)$ are respectively the actual fully unfolded distance and the predicted fully folded distance migrated at a given temperature (see Figure 1). However, complicating the analysis is the fact that the fully folded and fully unfolded distances migrated also increase as a function of temperature, giving rise to a background slope to the bands. To avoid the necessity of accounting for this slope, the fraction folded can be calculated as the linear combination of relative mobility values (R_fs) for the fully folded and unfolded states, which are constants—independent of temperature on these gels. In this "R_f method" P4−P6 mobility at each temperature is normalized to the mobility of the internal control molecule, BP 5/5a, and $R_f(T) = D_X(T)/D_U(T)$. The fraction folded is then calculated as $\alpha(T) = [R_f(T) - R_f(\text{fully unfolded})]/[R_f(\text{fully folded}) - R_f(\text{fully unfolded})]$. Since BP 5/5a is used for normalization, $R_f(\text{fully unfolded}) = 1$ (because both BP 5/5a and unfolded P4−P6 migrate at exactly the same rate), and the expression simplifies to $\alpha(T) = [R_f(T) - 1]/[R_f(\text{max}) - 1]$. For both methods the equilibrium constant observed at each temperature is $K_{eq} = \alpha/(1 - \alpha)$. Since $\Delta G = \Delta H - T\Delta S = -RT \ln K_{eq}$ and $\Delta H_{VH} = -R[\text{d} \ln K_{eq}/\text{d}(1/T)]$, $\Delta H^{\circ\prime}$ and $\Delta S^{\circ\prime}$ for the system can be extracted using a van't Hoff plot of $\ln K_{eq}$ vs $1/T$, where the slope = $-\Delta H^{\circ\prime}/R$ and the y-intercept = $\Delta S^{\circ\prime}/R$ ($\Delta H^{\circ\prime}$ and $\Delta S^{\circ\prime}$ are assumed to be independent of temperature).

For these experiments the distances that the BP 5/5a and the P4−P6 RNA bands moved at a given temperature were measured by using ImageQuanNT 4.1 software (Molecular Dynamics) to obtain vertical traces of PhosphorImager counts that started at the well and continued down the gel. The temperature in the gel at each trace was calculated by interpolating inward from the known end points of the linear gradient. Complicating the analysis of the gels is the downward sloping baseline caused by the increasing mobility of all bands as the gel temperature rises. The fraction folded was therefore calculated using both the baseline method and the R_f method. For the baseline method, a linear fit of several points in the low-temperature part of the P4−P6 band was used to predict the theoretical mobility of fully folded P4−P6 at higher temperatures (theoretical folded baseline, Figure 1B). The fraction folded, α, was calculated as $a/(a + b)$, where a equals the distance from the BP 5/5a band to the P4−P6 band, and $a + b$ is the distance from the BP 5/5a

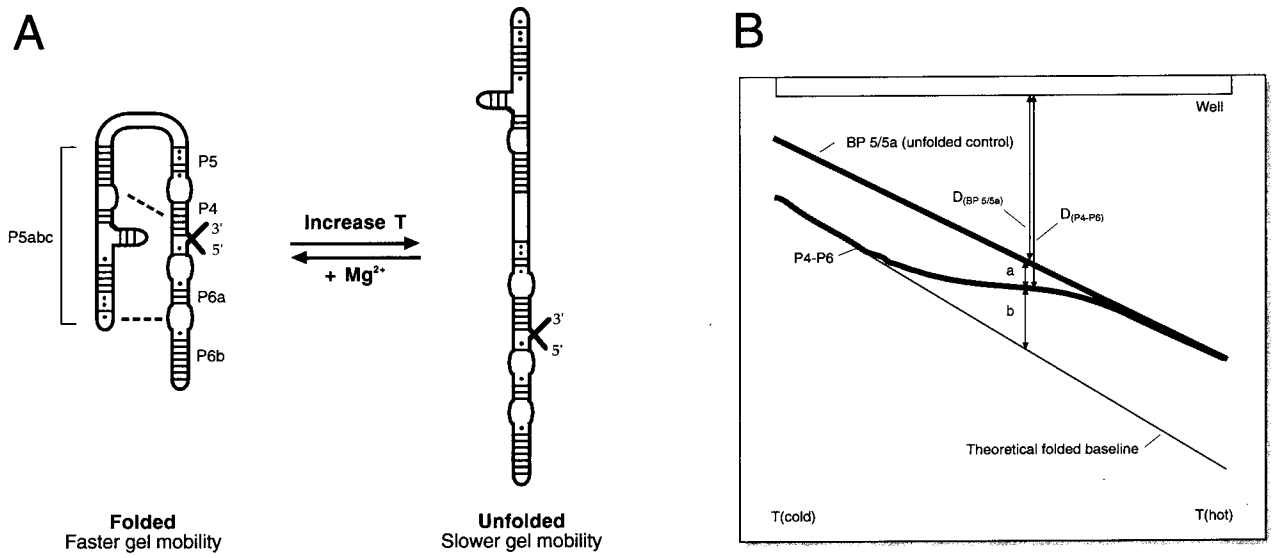

FIGURE 1: Analysis of P4−P6 mobility on temperature gradient gels. (A) Diagram of the interconversion between folded and unfolded forms of the P4−P6 tertiary structure. Shown here is a schematic diagram of the folding equilibrium for the P4−P6 RNA domain, labeled to indicate the P5abc subdomain and other helical elements. Evidence for this two-state equilibrium is discussed in Szewczak and Cech (*22*). Illustrated on the left is the compact, folded P4−P6 domain structure. On the right is a representation of the unfolded molecule, which is retarded relative to the folded molecule on nondenaturing polyacrylamide gels. The mutant molecule BP 5/5a is paired in the normally bent region between P5 and P5a and is incapable of forming the overall global tertiary fold, though it otherwise forms a normal secondary structure and P5abc subdomain fold (*21*). P4−P6 folding is stabilized by increasing concentrations of Mg^{2+} and destabilized by increased temperature. Intermediate mobilities result from the equilibrium between folded and unfolded states. (B) Diagram of an actual TGGE gel. The upper and lower dark lines represent the BP 5/5a and P4−P6 bands, respectively. The thin line marks the theoretical position of fully folded P4−P6, predicted from a linear fit of the low-temperature mobility of P4−P6. $D_{(BP\ 5/5a)}$ and $D_{(P4-P6)}$ correspond to the distances migrated by BP 5/5a and P4−P6 RNAs (used for R_f calculations) and have been offset for clarity. The baseline method uses measurements marked by a and b. See Experimental Procedures for details.

band to the theoretical position of fully folded P4−P6 (Figure 1B). For the R_f method, an R_f at a given temperature was calculated directly for P4−P6 by dividing the distance that the P4−P6 band migrated by the distance that BP 5/5a migrated, $D_{(P4-P6)}/D_{(BP\ 5/5a)}$ (Figure 1B). In both methods $K_{eq} = \alpha/(1 - \alpha)$ was then calculated for each temperature, and $\Delta H^{\circ\prime}$ and $\Delta S^{\circ\prime}$ were extracted from a linear fit of ln K_{eq} plotted as a function of $1/T$ (in K) over the range of α from 0.15 to 0.85 (to ensure that accurate K_{eq}s were calculated from the fraction folded, see Figure 3B).

Chemical Probing with DMS and CMCT. DMS modification experiments were performed following a modified version of established protocols (*34, 35*): First, two samples of 20 nM P4−P6 RNA in 300 μL of TGGE buffer and either 1 or 10 mM $MgCl_2$ (0.9 or 9.9 mM free Mg^{2+}) were annealed for 10 min at 55 °C and then left standing at room temperature for 20 min. Immediately afterward, each of the two RNA samples was in turn split into two 150 μL aliquots, one of which was equilibrated for 5 min at 14 °C and the other for 5 min at 60 °C. From each of these aliquots, 50 μL for a control "0 min" reaction without DMS was removed and directly added to 25 μL of DMS stop solution [0.5 M β-mercaptoethanol and 0.75 M sodium acetate (pH 5.5)] preequilibrated at the appropriate temperature. To initiate the actual modification reactions in the remaining 100 μL samples, 1 μL of a solution of 25% DMS in ethanol was added to each reaction tube. After 15 min of incubation, 50 μL from each reaction tube was removed and added to another tube at the same temperature containing 25 μL of DMS stop solution to quench the reaction. At 30 min the remaining 50 μL portion of each reaction mix was also quenched with 25 μL of stop solution. All experimental and control reaction tubes were held at the appropriate temperature for the full 30 min, to ensure that TGGE conditions were maintained for the entire time. At the completion of the experiment each sample was precipitated by the addition of 2.5 volumes of ethanol, and the RNA pellets were washed with 75% ethanol and air-dried before being redissolved in 10 μL of H_2O. DMS-containing samples were handled in the hood, and all pipet tips and tubes were treated with 5 M sodium hydroxide before disposal.

CMCT modification reactions were performed following a modified version of established protocols (*36*). First, P4−P6 was annealed at 55 °C and cooled to room temperature as for the DMS experiments. Next, 1 μM P4−P6 in 50 μL of TGGE buffer and the appropriate $MgCl_2$ concentration was preequilibrated at 14 or 60 °C for 5 min. To initiate the reactions a stock solution of either 42 or 84 mg/mL CMCT dissolved in TGGE/$MgCl_2$ buffer was added. Final concentrations of CMCT were 0, 1.68, 3.36, 6.72, and 16.8 mg/mL, and TGGE/$MgCl_2$ buffer was used to bring the final reaction volume for each sample up to 62.5 μL. All reactions were incubated for 60 min and then stopped by adding 78 μL (1.25 volume) of 0.5 M potassium borate (pH 6.1). Immediately afterward NaCl was added to a final concentration of 0.25 M and the RNA precipitated with 3 volumes of ethanol. RNA pellets were redissolved in 100 μL of H_2O.

Detection of Modified Bases by Primer Extension. Reverse transcription detection of modified bases was carried out essentially as described (*34, 35*). Samples containing approximately 0.3 pmol of DMS- or CMCT-treated RNA and 0.5 pmol of a 5′ ^{32}P-labeled DNA primer complementary to the 3′ end of the P4−P6 RNA were mixed in 6 μL of 50 mM Tris-HCl (pH 8.3), 60 mM NaCl, and 10 mM DTT and then annealed by heating for 1 min in a boiling water bath, followed by cooling to room temperature. Reverse transcrip-

tion reactions were carried out in a 5 μL volume containing 1 pmol of P4−P6 RNA, 1.67 pmol of primer, and 1 unit of AMV reverse transcriptase (Life Sciences) in 50 mM Tris-HCl (pH 8.3), 60 mM NaCl, 10 mM DTT, 6 mM MgOAc, and 80 μM each dNTP. Extension reactions were incubated at 37 °C for 15 min and then quenched by the addition of an equal volume of 95% formamide, 0.05% xylene cyanol, and 0.05% bromophenol blue. To localize the sites of modification, a set of dideoxy sequencing reactions (*37*) was also included. Samples were denatured by boiling for 1 min before being analyzed on 8% polyacrylamide−7 M urea sequencing gels, which were then dried on Whatman 3M paper and analyzed by scanning on a PhosphorImager (Molecular Dynamics). ImageQuanNT 4.1 software (Molecular Dynamics) was used to produce a trace of counts down the center of each DMS, CMCT, or sequencing lane. The traces were aligned manually without normalizing the peak intensities to produce the plots shown in Figure 5.

RESULTS

Temperature Gradient Gel Electrophoresis of the P4−P6 Domain RNA. To examine the state of the tertiary fold of P4−P6 as a function of temperature, we performed temperature gradient gel electrophoresis experiments under several different $MgCl_2$ concentrations. In 4.9 mM free Mg^{2+}, well above the concentration necessary to stabilize the P4−P6 tertiary structure (*10*), the P4−P6 and BP 5/5a RNAs travel at significantly different rates (Figure 2A). BP 5/5a migrates more slowly through the gel than P4−P6, which has a compact folded structure. The relative rate of migration ($D_{P4-P6}/D_{BP\ 5/5a}$) of both RNAs stays constant, and their mobilities do not appear to deviate from being a simple linear function of the temperature in the gel. We therefore infer that the P4−P6 domain structure is stable throughout this temperature range. At the opposite extreme, in 0.4 mM Mg^{2+}, P4−P6 and BP 5/5a comigrate through the TGGE gel over the range from 15 to 60 °C (Figure 2D). Because both RNAs exist in the same unfolded domain tertiary structure at this concentration of magnesium, the bands superimpose and are linear.

However, at intermediate concentrations of Mg^{2+} which are near to the $[Mg^{2+}]_{1/2}$ required for tertiary structure formation as observed by Fe(II)−EDTA probing (*10*), a melting transition can be seen for P4−P6 RNA. At 1.65 mM Mg^{2+}, for example, the mobility of P4−P6 at high temperatures begins to approach that of BP 5/5a (Figure 2B). Finally, a complete melt of the P4−P6 tertiary structure is recorded in a TGGE experiment with an effective concentration of 0.9 mM Mg^{2+} (Figure 2C). Over a temperature range of 15−60 °C the unfolded RNA control BP 5/5a still migrates at a rate which increases linearly as a function of temperature, but the mobility of P4−P6 RNA relative to this control changes dramatically. At 14 °C P4−P6 travels at a rate significantly faster than that of BP 5/5a. However, as the temperature in the gel rises, the mobility of P4−P6 decreases nonlinearly until, at high temperatures (above 50 °C), it travels at the same rate as, and is in fact coincident with, BP 5/5a. At 0.9 mM Mg^{2+} the midpoint of this transition on the TGGE gel, and thus the melting temperature of the global P4−P6 domain tertiary structure, is about 40 °C. We examined the melting behavior of P4−P6 under several buffer conditions and could observe the P4−P6 tertiary

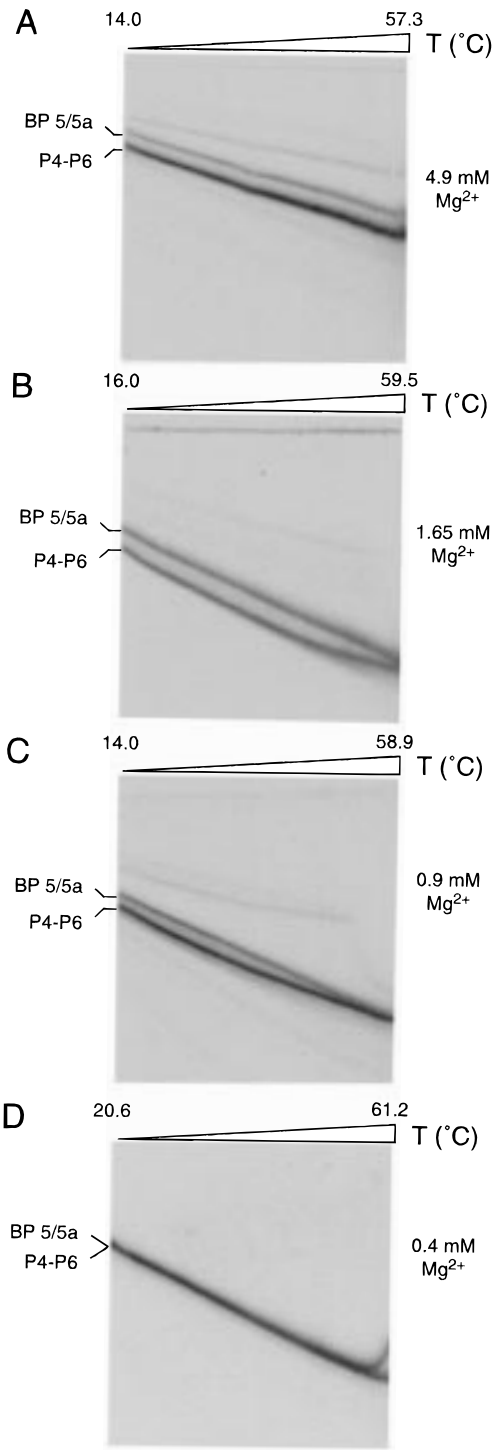

FIGURE 2: Temperature gradient gel electrophoresis of P4−P6 and BP 5/5a RNAs. TGGE experiments were carried out on 8% polyacrylamide gels with a horizontal linear temperature gradient of about 15−60 °C. For each gel the actual low and high temperatures were measured and are indicated on the left and right, respectively. See Experimental Procedures for details. (A) 4.9 mM Mg^{2+}: P4−P6 is completely folded over the entire temperature range of the gel, while BP 5/5a, the internal control, is unfolded. The relative rate of migration of P4−P6 and BP 5/5a remains constant over this temperature range. (B) 1.65 mM Mg^{2+}: P4−P6 RNA begins to unfold at high temperature. (C) 0.9 mM Mg^{2+}: at this Mg^{2+} concentration P4−P6 has a melting temperature of about 40 °C. (D) 0.4 mM Mg^{2+}: P4−P6 and BP 5/5a RNAs are both unfolded and have the same mobility. We have not investigated the sharp upward shift of one of the two RNA bands at very high temperature, but we believe it may be caused by melting of a secondary structure element in P4−P6 under extremely low salt conditions.

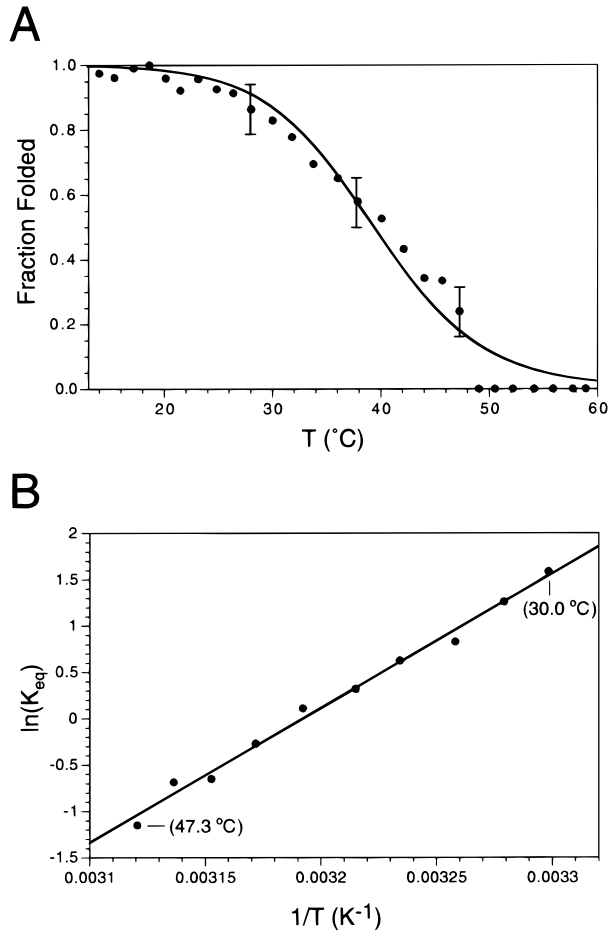

FIGURE 3: Thermodynamic calculations for formation of the P4−P6 tertiary structure at 0.9 mM Mg^{2+}. At each temperature the fraction of folded P4−P6 molecules was calculated as described in Experimental Procedures. (A) Plot of fraction folded vs temperature for the P4−P6 tertiary structure melting curve at 0.9 mM Mg^{2+}. Error bars represent an upper limit error estimate of ±10% in the measurement of fraction folded. For comparison, a fit of the data to a two-state transition has been included. (B) Van't Hoff plot for P4−P6 tertiary structure melt over the range where the fraction folded is between 0.15 and 0.85. The slope of the plot is $-\Delta H^{\circ\prime}/R$; the *y*-intercept is $\Delta S^{\circ\prime}/R$.

structure melt only over a rather narrow range of Mg^{2+} concentration. Below 0.7 mM Mg^{2+}, P4−P6 and BP 5/5a mobilities were identical at every temperature, and above 1.2 mM melting was not completed within the 14−60 °C temperature range attainable with our TGGE apparatus.

We interpret P4−P6 mobility at various temperatures as a linear combination of folded and unfolded mobilities (*22*). On the basis of this, we calculated the fraction of P4−P6 molecules folded and K_{eq} at a given temperature using the two methods described in Experimental Procedures. Representative fraction folded and van't Hoff plots are shown in Figure 3, and thermodynamic constants for three Mg^{2+} concentrations are summarized in Table 1. For the R_f method the T_m for the P4−P6 tertiary structure increases from 36 to 42 °C as the Mg^{2+} concentration is increased from 0.8 to 1.1 mM Mg^{2+}. From six duplicate TGGE experiments in 0.9 mM Mg^{2+}, we calculate thermodynamic parameters of $\Delta H^{\circ\prime} = -28 \pm 3$ kcal/mol and $\Delta S^{\circ\prime} = -91 \pm 8$ eu for the formation of the P4−P6 global tertiary structure. The baseline method of data analysis gave similar, though not identical, results, yielding melting temperatures which were about 5 °C lower than those obtained using the R_f method (Table 1). In addition, the baseline method had somewhat larger standard deviation among duplicate measurements. One reason for this is that the baseline method uses the beginning of the P4−P6 melting curve to predict the position of fully folded P4−P6, and this may introduce some error. The R_f method has the advantage of eliminating the need to fit a baseline. However, it makes the assumption that under a given set of buffer conditions the mobility of fully folded P4−P6 relative to BP 5/5a is a constant. This may not be exactly true, although it seems to be a very good approximation over the range of temperatures and with the resolution typical of these gels. It seems likely that the R_f method is the more accurate of the two.

Table 1: Thermodynamic Parameters for Formation of P4−P6 Tertiary Structure as a Function of Magnesium Concentration

	R_f method			baseline method		
$[Mg^{2+}]$ (mM)	T_m[a] (°C)	$\Delta H^{\circ\prime}$[a] (kcal/mol)	$\Delta S^{\circ\prime}$[a] (eu)	T_m[a] (°C)	$\Delta H^{\circ\prime}$[a] (kcal/mol)	$\Delta S^{\circ\prime}$[a] (eu)
0.8	36 ± 2	−38 ± 2	−126 ± 6	30 ± 3	−29 ± 3	−95 ± 11
0.9	39 ± 2	−28 ± 3	−91 ± 8	35 ± 5	−26 ± 5	−86 ± 15
1.1	42 ± 1	−25 ± 3	−78 ± 9	37 ± 2	−27 ± 2	−86 ± 7

[a] Errors reported are the standard deviation of either six (0.9 mM) or three (0.8 and 1.1 mM) independent measurements.

Chemical Probing Confirms That the TGGE Gel Mobility Change Is Due to the Melting of the P4−P6 Tertiary Structure. To verify that this change in P4−P6 mobility truly reflects melting of the molecule's tertiary structures, we probed the secondary and tertiary structure of P4−P6 RNA by treating the RNA with DMS and CMCT in gel buffer at temperatures equal to those at the low- and high-temperature points of the TGGE gels. Primer extension of treated RNA then reveals exposed bases by detecting DMS modifications at N1 of adenine and N3 of cytosine and CMCT modifications at N3 of uracil and N1 of guanine (*34*−*40*).

There are several well-characterized tertiary structure-specific DMS protections in P4−P6, most notably in the GAAA tetraloop and in the A-rich bulge (*10*, *21*). In 0.9 mM Mg^{2+} at 14 °C, weak DMS reactivity was seen for residues A151, A152, and A153, involved in tertiary interactions in the L5b tetraloop, and also at residues A183, A184, A186, and A187, in the A-rich bulge. A weak hit was also seen at A178. When the temperature was raised to 60 °C, the reactivity of these residues dramatically increased (see Figures 4 and 5). Similarly, a large increase in reactivity occurred at residues A225 and A226, which are known from the P4−P6 crystal structure to interact with the GAAA tetraloop (*6*). The pattern of reactivity of this entire set of residues shows clear evidence for melting of the tertiary structure of P4−P6 in 0.9 mM Mg^{2+} when the temperature is raised from 14 to 60 °C.

In addition to the residues involved in tertiary interactions that show a strong enhancement of reactivity at 60 °C, there are some positions that exhibit weak enhancement of reactivity at 60 °C. This second set of residues consists of nucleotides which are located near residues involved in tertiary interactions (A177, U182) or are located in weak secondary structure elements that flank internal loops within the molecule (G220, U221, U224). Other than the slight reactivity among this limited set of residues, we saw no evidence for disruption of the secondary structure of P4−

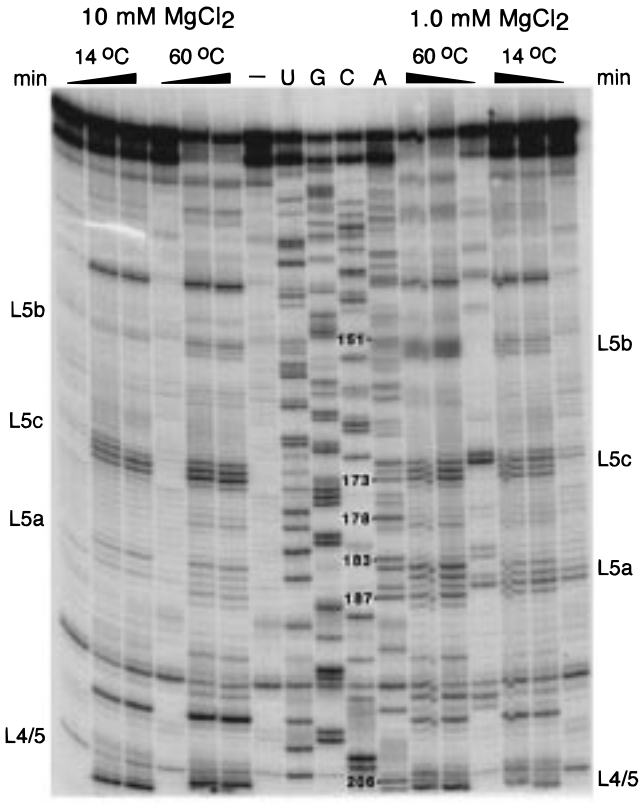

FIGURE 4: Representative dimethyl sulfate probing of P4−P6. P4−P6 RNA was probed in buffer containing 1× THE, 10 mM NaCl, and either 1 or 10 mM $MgCl_2$ (0.9 or 9.9 mM free Mg^{2+}). Reactions were carried out at 14 and 60 °C. Black wedges at the top of the gel indicate the increasing length of time of incubation (0, 15, and 30 min) for each DMS experiment. Loop regions of the P4−P6 secondary structure are labeled along the outside edge, and the positions of a few key residues are labeled in the center of the gel. Note that primer extension stops one residue prior to the modified base, so the bands in the probing lanes are shifted down one residue relative to the corresponding sequencing bands. (From left to right) Lanes 1−3: DMS probing of P4−P6 in TGGE buffer + 10 mM $MgCl_2$ at 14 °C. Lanes 4−6: DMS probing of P4−P6 in TGGE buffer + 10 mM $MgCl_2$ at 60 °C. Lane 7: untreated P4−P6 RNA control. Lanes 8−11: U-, G-, C-, and A-specific reverse transcription sequencing lanes. Lanes 12−14: DMS probing of P4−P6 in TGGE buffer + 1 mM $MgCl_2$ at 60 °C. Lanes 15−17: DMS probing of P4−P6 in TGGE buffer + 1 mM $MgCl_2$ at 14 °C.

P6 over the conditions tested. We also monitored the reactivity of residues known to be exposed to solvent in the folded structure, and as expected, they were reactive under all conditions. Finally, we probed P4−P6 at 14 and 60 °C in TGGE buffer + 10 mM $MgCl_2$. At this concentration there was no evidence for any disruption of the tertiary structure, consistent with the complete lack of a melt observed on TGGE gels at high Mg^{2+}.

Thus the DMS and CMCT probing experiments support our interpretation of the TGGE gels. In 0.9 mM Mg^{2+}, the tertiary structure of P4−P6 melts when the temperature is increased from 14 to 60 °C, with a T_m of about 40 °C. At 60 °C there appears to be some loosening of the structure around internal loops, but the vast majority of the secondary structure is unperturbed (Figure 6).

DISCUSSION

Our results show that temperature gradient gel electrophoresis can be extended to the analysis of the melting behavior of RNA tertiary structure. Using TGGE, we have observed a melting transition for the tertiary structure of P4−P6 under conditions of low ionic strength and millimolar concentrations of $MgCl_2$. The derived thermodynamic parameters demonstrate that tertiary folding is driven by enthalpy: $\Delta H^{\circ\prime}$ is clearly negative, about −30 kcal/mol, and $\Delta S^{\circ\prime}$ is also negative, about −90 eu, under these buffer conditions. There are, of course, advantages and disadvantages to using temperature gradient gel electrophoresis for studying structural transitions in nucleic acids. TGGE has the advantages that (1) it can be used to examine structural transitions in those cases where no UV signal can be observed, (2) only trace amounts of the radiolabeled material are required, and (3) it can be applied to any structural transition that results in a significant change in gel mobility. This last property is also a limitation, however. In addition, the use of gel electrophoresis limits the temperature range that can be observed and solvent conditions that can be used. This is the case for UV melting experiments as well, and the solution is to focus more on comparisons between molecules and to examine values obtained for $\Delta\Delta G$, $\Delta\Delta H$, and $\Delta\Delta S$. One other caveat is that the exact nature of the unfolded state of the molecule (in this case P4−P6 RNA) must be defined by other methods, such as the structure mapping employed here. We also used the internal unfolded control BP 5/5a, the mobility of which exactly matches unfolded P4−P6, which additionally helps to alleviate this problem.

For P4−P6 in particular, and for RNAs in general, tertiary structure stability is very sensitive to the concentration of Mg^{2+} ions (*9*, *41*−*43*). We see a very steep dependence of the P4−P6 tertiary structure T_m on $MgCl_2$ concentration. At a concentration of free Mg^{2+} less than 0.8 mM the structure is melted at all temperatures tested, while above 1.1 mM Mg^{2+} the structure remains folded through most or all of the temperature range. In 0.9 mM Mg^{2+} and low monovalent salt concentration, the P4−P6 global domain structure melts at about 40 °C and $\Delta H^{\circ\prime} = -28 \pm 3$ kcal/mol and $\Delta S^{\circ\prime} = -91 \pm 8$ eu for the folding transition. Thus the formation of the P4−P6 tertiary fold is enthalpically stabilized and has an unfavorable entropy term (disorder decreases upon folding). The sign and magnitude of these values are similar to those measured for formation of small tertiary structures such as tRNA and the 1051−1108 rRNA fragment (*2*, *44*, *45*) or for secondary structure elements such as short duplexes or small stem−loops (*46*, *47*). In contrast, the two tertiary structure interactions that have been studied extensively for the much larger group I intron, namely, P1 docking and GMP binding, are stabilized by a positive entropy term (*48*−*50*) (see Table 2). Because the docking or binding event itself must decrease the disorder of the system, displacement of ordered water molecules around solvated RNA functional groups or Mg^{2+} ions has been proposed to account for the positive ΔS (*48*−*50*), as has been reported for Mg^{2+} binding to ATP (*51*). One might have thought that P4−P6, with a large surface area buried by the formation of its tertiary structure (*6*), would also be stabilized by an entropic term, yet it is not.

Hydrogen bonds and stacking interactions stabilize RNA secondary structure formation by favorable enthalpic terms but have unfavorable entropic terms (*47*, *52*, *53*). Folding of P4−P6 also has a favorable ΔH term. There are several

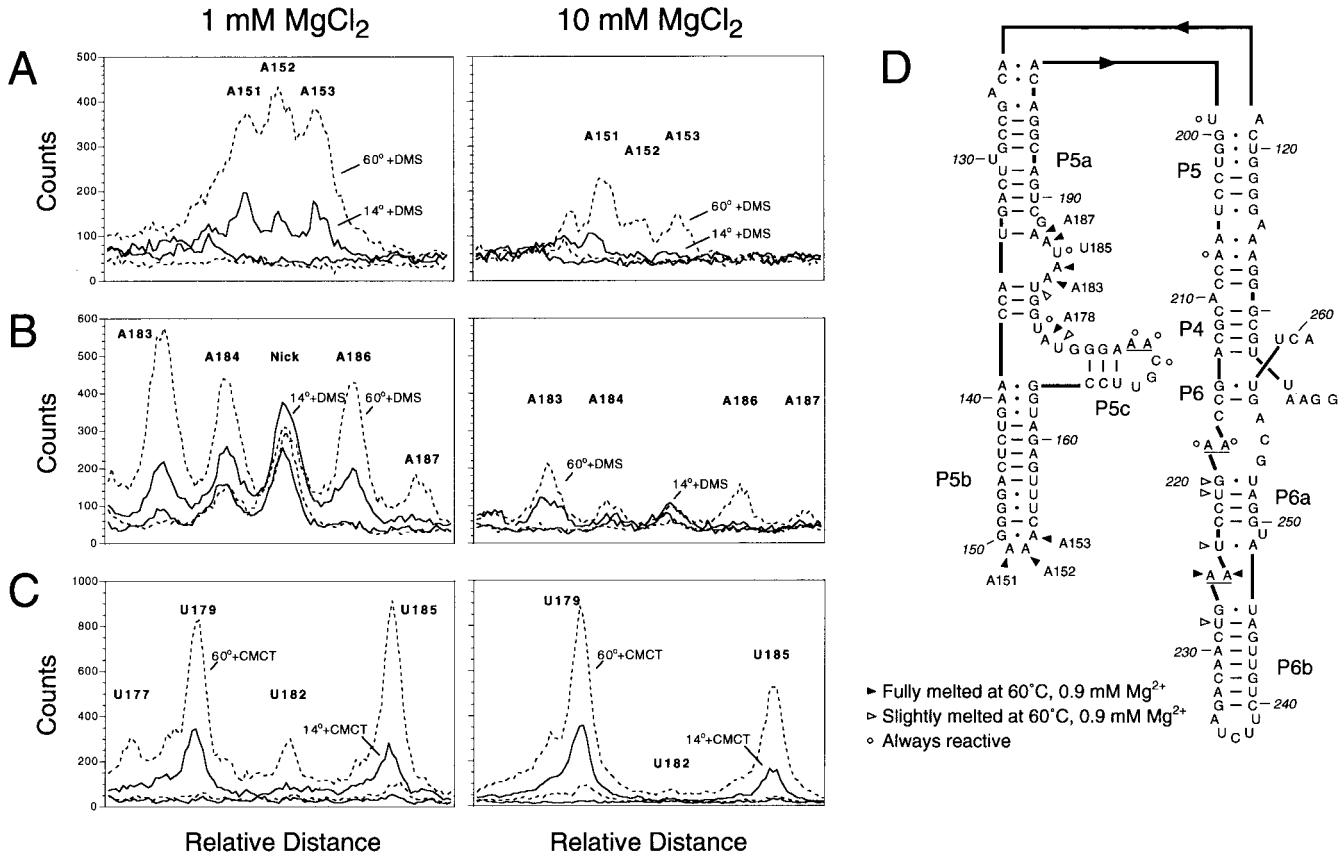

FIGURE 5: Chemical probing confirming that the P4−P6 tertiary structure is melted at 60 °C in 0.9 mM Mg^{2+}. Shown here are several PhosphorImager traces of chemical modification patterns detected by reverse transcription of P4−P6 RNA (see Experimental Procedures), along with a secondary structure diagram of P4−P6 summarizing the probing data. Solid and dashed lines indicate modification experiments carried out at 14 and 60 °C, respectively, and the amount of added $MgCl_2$ is indicated at the top. Reverse transcription of RNA incubated without the modification reagent was included in each set of experiments as a control for the background occurrence of transcription stops. For the data shown here the DMS incubation time was 15 min at both 14 and 60 °C. The CMCT concentration was 16.8 mg/mL for the 14 °C incubation and 1.68 mg/mL for the 60 °C incubation. (A) Pattern of dimethyl sulfate modification in the region from A151 to A153. (B) DMS modifications for A183 to A187. (C) CMCT modifications for residues U177 to U185. (D) Chemical probing data for residues 130−230 overlaid on the secondary structure of P4−P6. Filled triangles mark residues which show melting behavior (i.e., those that are reactive mainly at 60 °C in 0.9 mM free Mg^{2+}), and open triangles mark residues that only partially melt (i.e., those that are weakly reactive at 60 °C) in 0.9 mM Mg^{2+}. Open circles mark residues that are always unprotected. Residue numbering follows the standard *Tetrahymena* group I intron scheme (*54*), paired regions are labeled, and arrows mark 5′−3′ polarity. The three A-platforms (*7*) in the molecule are indicated by underlining.

Table 2: Thermodynamic Parameters for the Formation of P4−P6 Tertiary Structure Compared with Values for Other RNA Tertiary and Secondary Structures

RNA interaction	$\Delta H^{\circ\prime}$ (kcal/mol)	$\Delta S^{\circ\prime}$ (eu)
P4−P6 folding[a]	-28 ± 3	-91 ± 8
hairpin formation[b]	−44	−129
$tRNA^{fMet}$ tertiary structure[c]	−38	−116
group I intron G binding[d]	∼0	+23
group I intron P1 docking	+8[e]	+40[e]
	$+19 \pm 9$[f]	$+62 \pm 30$[f]

[a] This work, R_f method, 0.9 mM Mg^{2+}. [b] Example hairpin data were measured for the oligoribonucleotide 5′-GGACUUUUGUCC-3′ in 1 M NaCl, without Mg^{2+} by Antao and Tinoco (*46*). [c] Stein and Crothers (*41*). [d] McConnell and Cech (*49*). [e] Li et al. (*48*) studied over a temperature range of 10−25 °C. [f] Narlikar and Herschlag (*50*) studied over a temperature range of 30−60 °C.

likely reasons for this. First, the crystal structure of P4−P6 reveals a large number of potential hydrogen bonds that link the two halves of the molecule (*6*). Second, a number of stacking interactions occur, and the Mg^{2+} core interactions may be enthalpically stabilizing (*8*). Interestingly, P4−P6 molecules with mutations in the J5/5a region which substitute uracil residues for the wild-type sequence appear to have an enthalpic term near zero (A. A. Szewczak and T. R. Cech, unpublished results), suggesting that the J5/5a region may contribute some favorable enthalpy. In contrast, ΔH for GMP binding is near zero and for P1 docking is actually positive (Table 2). G binding results in the formation of a few hydrogen bonds and only minimal stacking. P1 docking involves more hydrogen bonds than G binding, but not nearly as many as P4−P6-folding, and little or no stacking. Thus, enthalpic terms are much less stabilizing for these interactions.

It has been suggested that early steps in RNA folding may not be associated with positive entropy terms due to the absence of prebound water molecules and because of the early formation of ordered structural elements required for hydrogen bonding and stacking within the RNA (*50*). In contrast, late RNA folding events such as true tertiary structure formation, involving assembly of predominantly prefolded structural elements, may be associated with positive entropy terms (*50*). This is certainly consistent with what has been observed for P1 docking and G binding (*48*−*50*). P4−P6 formation is a late folding event in the sense that its

FIGURE 6: Melting behavior of chemical modifications mapped on the three-dimensional structure of P4−P6. Residues that are protected at 14 °C but are strongly reactive at 60 °C are marked in dark blue. Residues that are only weakly reactive at 60 °C are colored green. Red indicates residues that are always reactive because their functional groups are exposed to solvent. The remaining light blue residues are unreactive at all temperatures, indicating that the P5abc subdomain fold and the vast majority of the molecule's secondary structure are unperturbed in the TGGE experiments. The stick representation of P4−P6 RNA and the overlaid nucleic acid backbone ribbon were drawn using Insight II (Biosym), and atomic coordinates are from Cate et al. (*6*).

secondary structure and P5abc subdomain fold are already fully formed. Yet the P4−P6 domain tertiary fold has an unfavorable entropic term. Thus the interacting forces driving the formation of RNA tertiary structures may defy simple categorization. It appears that RNA tertiary structure can be stabilized by a mix of enthalpic and entropic terms, depending on the details of the system, and in the case of this particular RNA domain, the tertiary fold is stabilized by a favorable ΔH term of about −30 kcal/mol.

ACKNOWLEDGMENT

T7 RNA polymerase was generously provided by Anne Gooding. We thank Lara Weinstein for helpful comments on the manuscript.

REFERENCES

1. Atkins, J. F., and Gesteland, R. F. (1993) *The RNA World*, Cold Spring Harbor Laboratory Press, Plainview, NY.
2. Draper, D. E. (1996) *Trends Biochem. Sci. 21*, 145−149.
3. Zarrinkar, P. P., and Williamson, J. R. (1996) *Nat. Struct. Biol. 3*, 432−438.
4. Strobel, S. A., and Doudna, J. A. (1997) *Trends Biochem. Sci. 22*, 262−266.
5. Doudna, J. A., and Doherty, E. A. (1997) *Folding Des. 2*, 65−70.
6. Cate, J. H., Gooding, A. R., Podell, E., Zhou, K., Golden, B. L., Kundrot, C. E., Cech, T. R., and Doudna, J. A. (1996) *Science 273*, 1678−1685.
7. Cate, J. H., Gooding, A. R., Podell, E., Zhou, K., Golden, B. L., Szewczak, A. A., Kundrot, C. E., Cech, T. R., and Doudna, J. A. (1996) *Science 273*, 1696−1699.
8. Cate, J. H., Hanna, R. L., and Doudna, J. A. (1997) *Nat. Struct. Biol. 4*, 553−558.
9. Latham, J. A., and Cech, T. R. (1989) *Science 245*, 276−282.
10. Murphy, F. L., and Cech, T. R. (1993) *Biochemistry 32*, 5291−5300.
11. Michel, F., and Westhof, E. (1990) *J. Mol. Biol. 216*, 585−610.
12. Laggerbauer, B., Murphy, F. L., and Cech, T. R. (1994) *EMBO J. 13*, 2669−2676.
13. Doherty, E. A., and Doudna, J. A. (1997) *Biochemistry 36*, 3159−3169.
14. van der Horst, G., Christian, A., and Inoue, T. (1991) *Proc. Natl. Acad. Sci. U.S.A. 88*, 184−188.
15. Zarrinkar, P. P., and Williamson, J. R. (1994) *Science 265*, 918−924.
16. Downs, W. D., and Cech, T. R. (1996) *RNA 2*, 718−732.
17. Sclavi, B., Woodson, S., Sullivan, M. R., and Brenowitz, M. (1997) *J. Mol. Biol. 266*, 144−159.
18. Sclavi, B., Sullivan, M., Chance, M. R., Brenowitz, M., and Woodson, S. A. (1998) *Science 279*, 1940−1943.
19. Doudna, J. A., and Cech, T. R. (1995) *RNA 1*, 36−45.
20. Murphy, F. L., Wang, Y. H., Griffith, J. D., and Cech, T. R. (1994) *Science 265*, 1709−1712.
21. Murphy, F. L., and Cech, T. R. (1994) *J. Mol. Biol. 236*, 49−63.
22. Szewczak, A. A., and Cech, T. R. (1997) *RNA 3*, 838−849.
23. Creighton, T. E. (1979) *J. Mol. Biol. 129*, 235−264.
24. Fischer, S. G., and Lerman, L. S. (1983) *Proc. Natl. Acad. Sci. U.S.A. 80*, 1579−1583.
25. Fischer, S. G., and Lerman, L. S. (1979) *Cell 16*, 191−200.
26. Thatcher, D. R., and Sheikh, R. (1981) *Biochem. J. 197*, 111−117.
27. Thatcher, D. R., and Hodson, B. (1981) *Biochem. J. 197*, 105−109.
28. Wartell, R. M., Hosseini, S. H., and Moran, C. P., Jr. (1990) *Nucleic Acids Res. 18*, 2699−2705.
29. Rosenbaum, V., and Riesner, D. (1987) *Biophys. Chem. 26*, 235−246.
30. Riesner, D., Steger, G., Zimmat, R., Owens, R. A., Wagenhofer, M., Hillen, W., Vollbach, S., and Henco, K. (1989) *Electrophoresis 10*, 377−389.
31. Latham, J. A., Zaug, A. J., and Cech, T. R. (1990) *Methods Enzymol. 181*, 558−569.
32. Marky, L. A., and Breslauer, K. J. (1987) *Biopolymers 26*, 1601−1620.
33. Puglisi, J. D., and Tinoco, I., Jr. (1989) *Methods Enzymol. 180*, 304−325.
34. Inoue, T., and Cech, T. R. (1985) *Proc. Natl. Acad. Sci. U.S.A. 82*, 648−652.
35. Zaug, A. J., and Cech, T. R. (1995) *RNA 1*, 363−374.
36. Jabri, E., Aigner, S., and Cech, T. R. (1997) *Biochemistry 36*, 16345−16354.
37. Saenger, F., Nicklen, S., and Coulson, A. R. (1977) *Proc. Natl. Acad. Sci. U.S.A. 74*, 5463−5467.
38. Lawley, P. D., and Brookes, P. (1963) *Biochem. J. 89*, 127−138.
39. Jones, J. W., and Robins, R. K. (1963) *J. Am. Chem. Soc. 85*, 193−201.
40. Ho, N. W. Y., and Gilham, P. T. (1967) *Biochemistry 6*, 3632−3639.

41. Stein, A., and Crothers, D. M. (1976) *Biochemistry 15*, 160−168.
42. Celander, D. W., and Cech, T. R. (1991) *Science 251*, 401−407.
43. Pan, T. (1995) *Biochemistry 34*, 902−909.
44. Crothers, D. M., Cole, P. E., Hilbers, C. W., and Shulman, R. G. (1974) *J. Mol. Biol. 87*, 63−88.
45. Lu, M., and Draper, D. E. (1994) *J. Mol. Biol. 244*, 572−585.
46. Antao, V. P., and Tinoco, I. J. (1992) *Nucleic Acids Res. 20*, 819−824.
47. Serra, M. J., and Turner, D. H. (1995) *Methods Enzymol. 259*, 242−261.
48. Li, Y., Bevilacqua, P. C., Mathews, D., and Turner, D. H. (1995) *Biochemistry 34*, 14394−14399.
49. McConnell, T. S., and Cech, T. R. (1995) *Biochemistry 34*, 4056−4067.
50. Narlikar, G. J., and Herschlag, D. (1996) *Nat. Struct. Biol. 3*, 701−710.
51. Banyasz, J. L., and Stuehr, J. E. (1973) *J. Am. Chem. Soc. 95*, 7226−7231.
52. Turner, D. H., Sugimoto, N., Kierzek, R., and Dreiker, S. (1987) *J. Am. Chem. Soc. 109*, 3783−3785.
53. Freier, S. M., Alkema, D., Sinclair, A., Neilson, T., and Turner, D. H. (1985) *Biochemistry 24*, 4533−4539.
54. Cech, T. R., Damberger, S. H., and Gutell, R. R. (1994) *Nat. Struct. Biol. 1*, 273−280.

BI980633E